Effect of Print Masks on the Functional Performance of Inkjet Printed Pd Hexadecanethiolate in Toluene

J. William Boley, ChenChao Shou, Patrick McCarthy, Timothy Fisher, and George T.C.-Chiu; Purdue University; West Lafayette, IN/USA

Abstract

For more than a decade studies have shown that print masks can be designed to alleviate print artifacts in inkjet printed images by using the ability to independently address multiple nozzles within a print-head. With the increase in applications of inkjet functional printing in recent years, the higher throughput associated with multiple nozzle arrays is necessary for large scale production. This provides the motivation for designing print masks that can maximize the quality of inkjet printed devices rather than minimize the number of print artifacts detectable by the human eye. Four separate print masks are selected and employed for printing a rectangle onto Silicon and a six-contact bridge-type pattern onto oxidized Silicon using a Pd ink. The resulting printed rectangles are compared via image quality metrics while the six-contact bridge-type patterns were characterized electrically and compared via sheet resistance. The results show a clear trend. The print masks showing better performance via image quality metrics also showed better performance in terms of sheet resistance.

Introduction

Many print-heads today consist of multiple nozzles. As one can expect, arrays of multiple nozzles lead to higher throughput because they provide the ability to simultaneously deposit ink at multiple locations. With the drastic increase in functional inkjet printed devices over the past decade [1–10], the throughput associated with multiple nozzle arrays is necessary for large scale manufacturing. Figure 1 shows a schematic of a print-head array consisting of k nozzles. The column on the left is made up of odd numbered nozzles while the column on the right is comprised of even numbered nozzles. The columns are separated by a distance a in the print-head scan direction and the distance between nozzles in the media advance direction is b.

In an ideal situation, the print-head would travel over the media in the print-head scan direction until reaching the width of the image, advance the length of the print-head ($b \cdot k$) in the media advance direction, and repeat this process until reaching the end of the image (i.e. the print-head would visit each pixel of the image once and only once). However, hardware limitations and print quality requirements make it difficult to print from all nozzles or even adjacent nozzles at a given time. Thus, print modes are established to trade-off between print speed and print quality requirements based on different media, ink, and image content. For example, a multiple-pass print mode optimized for halftoned images may not be desirable or have adequate throughput for text or line art documents, which have higher requirements on swath alignment.

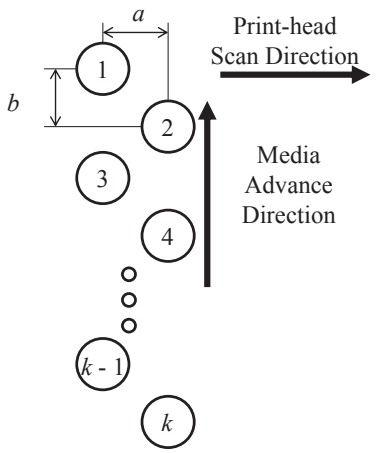

Figure 1. *Schematic of an array of k nozzles with the print-head scan direction and the media advance direction defined.*

Since not all nozzles should be fired at any given pass for a multiple-pass print mode, the print-head must pass over each pixel more than once so that there is more than one opportunity for ink deposition. Figure 2 shows how an image can be printed by two passes of a print-head with six nozzles. The top left image of Figure 2 is the image to be printed. On the first pass, the bottom three nozzles pass over the image filling in the top left pixel with the fourth nozzle, the middle pixel with the fifth nozzle, and the bottom right pixel with the sixth nozzle (i.e. all of the pixels requiring ink which are labeled with pass number 1) as shown in the bottom left image of Figure 2. The substrate then moves three nozzles in the media advance direction relative to the print-head. The print-head then passes over the image pixels its second and final time, printing the top middle pixel from the first nozzle and the middle left pixel from the second nozzle (i.e. all of the pixels requiring ink which are labeled with pass number Figure 2) as illustrated in the bottom right image of Figure 2. The top right image of Figure 2 is the print mask (*PM*) used for printing the image. The specific *PM* shown in Figure 2 is referred to in the literature [11, 12] as the checkerboard design because of the checkerboard pattern of 1's and 2's in the *PM*. The checkerboard *PM* design is often used to avoid consecutive firing of the same nozzle and in some cases to avoid print artifacts. Due to hardware limitations and print quality requirements, *PM*s other than that of the checkerboard design may be needed.

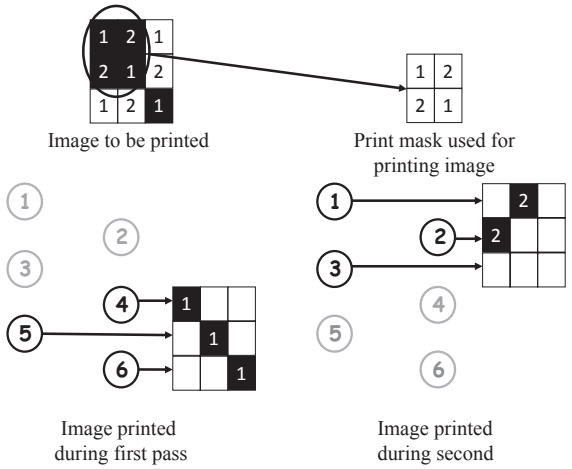

Figure 2. *Example of printing an image with two passes of a print-head.*

Existing Print Mask Literature

In 1999, Yen et al. [11] introduced two methods for *PM* design. First, in order to produce an imperceptible (by the human visual system) printed pattern that covers up banding artifacts caused by defective print-head nozzles, a two-pass 4 by 4 *PM* with triangular clusters, derived from halftoning techniques [13], was used. Second, an alternative *PM* was derived from generating a super smooth dithering matrix [14], which proved to address artifacts associated with ink migration by guiding the ink migration into a super smooth dithering pattern undetectable by the human eye. Subsequently, Yen et al. [12] formulated the automatic selection of a *PM* as a general constrained optimization problem applicable to multiple-pass print modes for multiple-level (multiple drops per pixel), multiple-drop (multiple drops per pixel, per pass) technologies. The method begins with a random initial solution found by means of a greedy algorithm, followed by neighborhood search techniques. However, no specific guidelines were given to consider drop placement error, which can be on the same order of magnitude as the drop radius [4, 10, 15], or to consider the occurrence of coalescence between neighboring drops, which affects the performance of printed electronics, especially with solvents exhibiting high vapor pressures and ink/substrate systems exhibiting non-zero receding contact angles [16].

Contributions Regarding Print Mask Design

This study builds upon our previous work by measuring device performance of patterns printed using different PMs. In this work, four separate PMs are employed for functional printing. First, each of the PMs is used to print a single layered rectangle onto an Si substrate. Upon obtaining optical micrographs, image quality metrics are employed to demonstrate that each of the four PMs will generate different results. The image quality metrics used to analyze each printed rectangle are fill, a modified version of mottle, and raggedness. Next, each of the PMs is used to print a ten layer four probe pattern of palladium hexadecanthiolate onto oxidized silicon substrates. The printed patterns are then electrically characterized upon thermolysis.

Results and Discussion

The print mode parameters constant for all image quality experiments are as follows:

- Print-head scan speed: 1mm/s
- Unidirectional printing
- Media advance speed: 1mm/s
- Print-head return speed: 45mm/s
- Nozzle resolution: $b = 70.25\mu$m
- Image resolution: 70.25μm/pixel
- Ink: 32mM solution of Pd hexadecanethiolate in toluene
- Image: 15×8 filled rectangle for image metrics performance and a six-contact, bridge-type pattern for functional performance (see Figure 5)
- Substrate: Si for printed rectangle and Si/O_2 for functional performance
- Distance between nozzle columns: $a = 266.01\mu$m
- Print Mask size: 4 rows $\times 4$ columns

The *PM*s chosen for this study were

$$PM_2 = \begin{pmatrix} 1 & 2 & 1 & 2 \\ 1 & 2 & 2 & 1 \\ 2 & 1 & 2 & 1 \\ 2 & 1 & 1 & 2 \end{pmatrix}, PM_3 = \begin{pmatrix} 1 & 2 & 1 & 3 \\ 1 & 2 & 3 & 1 \\ 3 & 1 & 3 & 2 \\ 3 & 1 & 2 & 1 \end{pmatrix},$$

$$PM_4 = \begin{pmatrix} 4 & 2 & 4 & 2 \\ 3 & 1 & 2 & 4 \\ 2 & 4 & 1 & 4 \\ 1 & 3 & 4 & 1 \end{pmatrix}, \text{ and } PM_6 = \begin{pmatrix} 2 & 5 & 2 & 6 \\ 1 & 5 & 1 & 5 \\ 6 & 5 & 2 & 4 \\ 1 & 5 & 1 & 3 \end{pmatrix};$$

where the subscript for each PM_i denotes the number of passes.

At this point a guide should be given on how to interpret the resulting print masks. It can be observed especially in PM_4 and PM_6 that some pass numbers only appear once or twice in the print mask (3 for PM_4 and 3 and 4 for PM_6). This low occurrence of pass numbers translates to low ejection frequencies for the corresponding nozzles. If the ejection frequencies are too low, then these nozzles will clog as the solvent around the orifice dries allowing for solute to build up. In general, this should be addressed. However, for this study, no resulting clogging issues were directly observed.

Image Quality Results for a Printed Rectangle

Image Quality Metrics Employed

There are many attributes given in [17, 18] that measure the quality of a given image. Rather than including all measures, three attributes naturally thought to be indicative of device performance were chosen from [17]. These three image quality attributes are mottle, raggedness, and fill. This section gives a brief description of these attributes and discusses how they can relate to functional printing.

Mottle. Mottle as defined in [17] as irregular spatial patterns with frequencies less than 0.4 cycles per *mm* in every direction. To compute mottle, the region of interested as defined by [17] is divided into at least 100 uniform, non-overlapping square tiles.

The mottle is then obtained by taking the standard deviation of the average optical density over all tiles. Further investigation conducted by Smith, Brown, and Brown [19] has shown that mottle can be reported in terms of the grayscale value (GSV), mottle is a function of the tile size, and that mottle is an indicator of the occurrence of coalescence within an image [19]. Thus, the method proposed in [19] has been chosen to measure *PM* quality in this paper.

Raggedness. Raggedness is described in [17] as the standard deviation of the residual error perpendicular to the best fit edge threshold. This attribute was chosen because the raggedness of a line can affect the performance of a printed device (e.g., two adjacent conductive traces in close proximity are less likely intersect if they have low raggedness).

Fill. The third attribute used in this study is fill. It is defined [17] as the ratio of the area within the region of interest that has a relative reflectance of at least 75% to the total area of the region of interest. Fill is a measure of image homogeneity, which is important in printed devices such as printed circuits and displays [20].

Results

Images of the resulting printed rectangles are featured in Figure 3. It is clear qualitatively that ink migration is drastically reduced as the number of passes increases. This is a result from the drying time associated with adjacently deposited drops, which increases for the selected print masks as the number of passes increases, thus decreasing the occurrence of drop coalescence. The resulting image quality metrics summarized in Table 1 and fig. 4 further validate this observation.

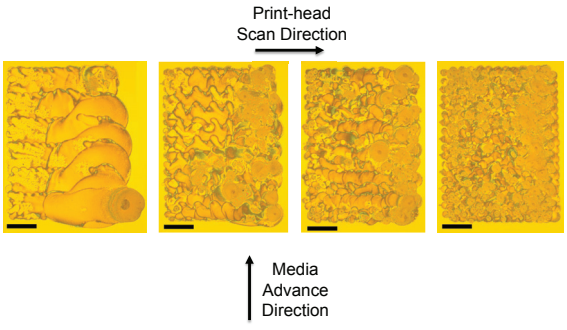

Figure 3. *Resulting printed rectangles, each printed by a different PM. Printed by (left to right): PM_2, PM_3, PM_4, and PM_6. Scale bars are 500μm in length.*

Resulting image quality metrics corresponding to print masks.

	PM_2	PM_3	PM_4	PM_6
Raggedness(μm)	85	66	26	19
Fill	0.26	0.15	0.11	0.06

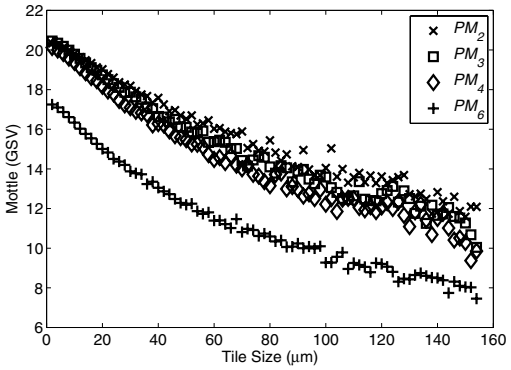

Figure 4. *Resulting mottle at different tile sizes.*

Functional Performance of a Six-Contact Bridge-Type Pattern

The six-contact bridge-type input image featured in Figure 5 was printed using each of the four print masks (PM_2, PM_3, PM_4, and PM_6), each consisting of ten layers. The resulting printed patterns are shown in Figure 6. The resulting measured sheet resistances obtained from each of the printed patterns are summarized in Table 2. As evident, the high occurrence of film non-uniformities from the patterns printed by PM_2 and PM_3 leads to open circuits during the thermolosys process, resulting in an undetectable amount of current passing between the printed pads. However, electricity appears to conduct for patterns printed using PM_4 and PM_6. Comparing the electrical measurements of PM_4 and PM_6 shows an order of magnitude decrease in sheet resistance as well as improvement of measurement uncertainty by more than two-fold when going from PM_4 to PM_6.

One may wonder if increasing the number of passes to 12 would further improve the functional performance. This question can be addressed by using the data obtained from the previous studies involving printed Pd hexadecanthiolate [6, 21]. For the prior work the minimum deposition time difference was several seconds (orders of magnitude larger than the evaporation time for a drop [22]). Therefore, it is expected that a well performing print mask should be comparable to the prior work. Assuming a constant packing factor for the solute, the line thickness for the 4-probe pattern printed by PM_6 can be approximated by $50\text{nm}\left(\frac{32\text{mM}}{50\text{mM}}\right)\left(\frac{10\text{layers}}{5\text{layers}}\right)\left(\frac{70.25\mu\text{m}}{100\mu\text{m}}\right) \approx 45\text{nm}$. This results in a resistivity of approximately $1.12 \times 10^{-6}\Omega$m, which is actually smaller than the previous study by a factor of 4, indicating that a print mask with a larger number of total passes would not give a better result.

Further comparison to previous work can be made through the time required for printing. A six pass print mask has half the required print time of a 12 pass, which is equivalent to a single nozzle advancement. Furthermore, the previous work did not print adjacent drops on a single pass, resulting in four total passes for a single layer. Therefore, using a 12 nozzle print-head and printing with PM_6 results in a printing time smaller than the previous work by a factor of approximately 8.

One thing left to compare is the print time for a single pass print

mode with that of a six pass print mode. All things equal, the print speed for a single pass print mode requires a maximum print-head scan speed of 0.23mm/s to obtain a similar electrical performance [23]. However, this would result in a print time 0.7 times that of the six pass print mode, thus generating similar performance in less time. However, the maximum resulting frequency would be about 3Hz in the case of a single pass, increasing the likelihood of nozzle clogging. Therefore, future work should be conducted to determine an optimal printing frequency range.

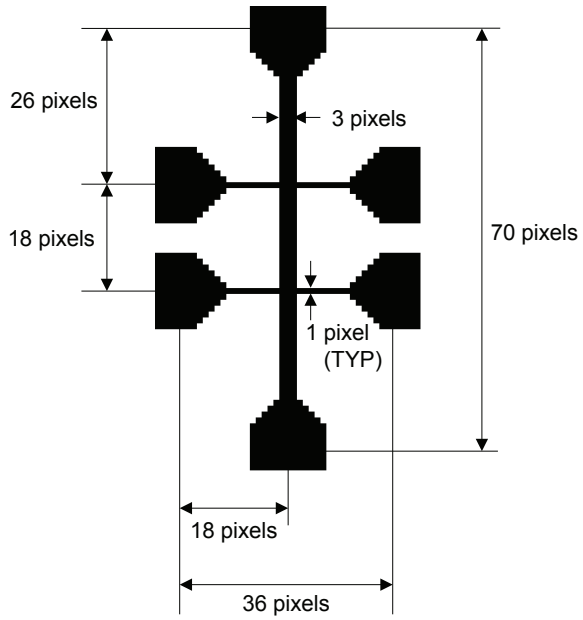

Figure 5. *Target six-contact bridge-type pattern with pertinent dimensions labeled (Note:* $1 pixel = 70.25 \mu m$*).*

Resulting sheet resistances $(\Omega/\square)$ **corresponding to optimal print masks. N/A corresponds to samples exhibiting no measurable current.**

PM_2	PM_3	PM_4	PM_6
N/A	N/A	$178 \pm 8.7\%$	$25 \pm 3.8\%$

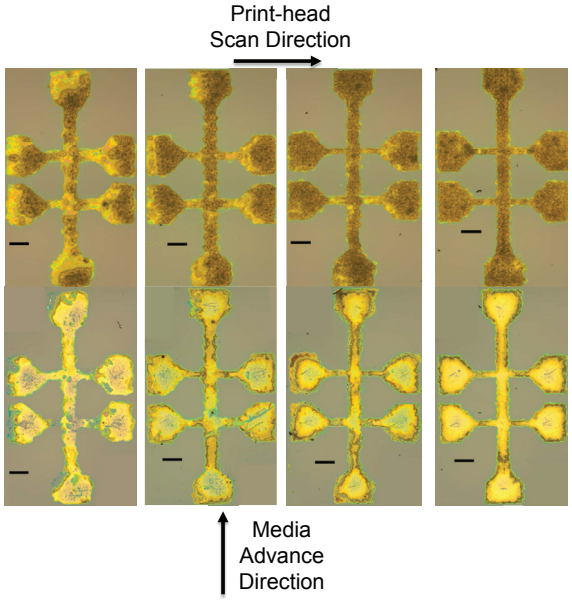

Figure 6. *Resulting printed six-contact bridge-type patterns, each printed by a different* PM*. Printed by (left to right):* PM_2*,* PM_3*,* PM_4*, and* PM_6*. Top row shows micrographs of printed patterns prior to thermolosys. Bottom row shows micrographs post thermolosys and after electrical characterization. Scale bars are* $500 \mu m$ *in length.*

References

[1] Calvert, P., 2001. "Inkjet printing for materials and devices". *Chemistry of Materials,* **13**(10), Oct, pp. 3299–3305.

[2] Shimoda, T., Morii, K., Seki, S., and Kiguchi, H., 2003. "Inkjet printing of light-emitting polymer displays". *MRS Bulletin,* **28**(11), Nov, pp. 821–827.

[3] de Gans, B., Duineveld, P., and Schubert, U., 2004. "Inkjet printing of polymers: State of the art and future developments". *Advanced Materials,* **16**(3), Feb 3, pp. 203–213.

[4] Burns, S., Cain, P., Mills, J., Wang, J., and Sirringhaus, H., 2003. "Inkjet printing of polymer thin-film transistor circuits". *MRS Bulletin,* **28**(11), Nov, pp. 829–834.

[5] Subramanian, V., Chang, P., Lee, J., Molesa, S., and Volkman, S., 2005. "Printed organic transistors for ultra-low-cost RFID applications". *IEEE Transactions on Components and Packaging Technologies,* **28**(4), Ded, pp. 742–747. 10th Therminic Workshop, Sophia Antipolis, France, Sep 29-Oct 01, 2004.

[6] Bhuvana, T., Boley, W., Radha, B., Dolash, B. D., Chiu, G., Bergstrom, D., Reifenberger, R., Fisher, T. S., and Kulkarni, G. U., 2010. "Inkjet printing of palladium alkanethiolates for facile fabrication of metal interconnects and surface-enhanced Raman scattering substrates". *Micro & Nano Letters,* **5**(5), Oct, pp. 296–299.

[7] Singh, M., Haverinen, H. M., Dhagat, P., and Jabbour, G. E., 2010. "Inkjet Printing-Process and Its Applications". *Advanced Materials,* **22**(6), Feb 9, pp. 673–685.

[8] Kumar, V., Boley, J. W., Yang, Y., Ekowaluyo, H., Miller, J. K., Chiu, G. T. C., and Rhoads, J. F., 2011. "Bifurcation-based mass sensing using piezoelectrically-actuated microcantilevers". *Applied Physics Letters,* **98**(15), Apr 11.

[9] Derby, B., and Reis, N., 2003. "Inkjet printing of highly loaded particulate suspensions". *MRS Bulletin,* **28**(11), Nov, pp. 815–818.

[10] Derby, B., 2008. "Bioprinting: inkjet printing proteins and hybrid cell-containing materials and structures". *Journal of Materials Chemistry,* **18**(47), pp. 5717–5721.

[11] Yen, J., Lin, Q., and Wong, P., 1999. Print masks for inkjet printers. US Patent 5,992,962.

[12] Yen, J., Carlsson, M., Chang, M., Garcia, J., and Nguyen, H., 2000. "Constraint solving for inkjet print mask design". *Journal of Imaging Science and Technology,* **44**(5), Sep-Oct, pp. 391–397.

[13] Bayer, B., 1973. "An Optimum Method for Two-Level Rendition of Continuous-Tone Pictures". *Research Laboratories, Eastman Kodak Company*, pp. 26–11 – 26–15.

[14] Ulichney, R., 1993. "The Void-and-Cluster Method for Dither Array Generation". *SPIE,* **1913**, pp. 332–343.

[15] de Gans, B., and Schubert, U., 2003. "Inkjet printing of polymer micro-arrays and libraries: Instrumentation, requirements, and perspectives". *Macromolecular Rapid Communications,* **24**(11), Jul 25, pp. 659–666.

[16] "To be published".
[17] ISO/IEC/ 13660 draft standard, information technology office equipment - measurement of image quality attributes for hardcopy output - binary monochrome text and graphic images.
[18] Shaw, R., 1997. "Image Quality Considerations for Printing Digital Photographs". 13th International Conference on Digital Printing Technologies, Minneapolis, MN, OCT 2-6.
[19] Jones, N., Sargeant, S. J., and Sargeant, K., 1998. "Characterizing and Modeling Coalescence in Inkjet Printing". 14th International Conference on Digital Printing Technologies, Toronto, Ontario, Canada, Oct 18-23.
[20] Soltman, D., Smith, B., Kang, H., Morris, S. J. S., and Subramanian, V., 2010. "Methodology for Inkjet Printing of Partially Wetting Films". *Langmuir,* **26**(19), Oct 5, pp. 15686–15693.
[21] Boley, W., Bhuvana, T., Hines, B., Sayer, R. A., Chiu, G., Fisher, T. S., Bergstrom, D., Reifenberger, R., and Kulkarni, G. U., 2009. "Inkjet Printing Involving Palladium Alkanethiolates and Carbon Nanotubes Functionalized with Single-Strand DNA". In NIP 25: Digital Fabrication 2009, Technical Program and Proceedings, Soc Imaging Sci & Technol; Imaging Soc Japan, pp. 824–827. 25th International Conference on Digital Printing Technologies, Louisville, KY, Sep 20-24, 2009.
[22] Boley, J. W., 2013. "Print mask design for inkjet functional printing". PhD thesis, Purdue University, May.
[23] Boley, J. W., Chou, C., McCarthy, P., Fisher, T. S., and Chiu, G., 2013. "The Role of Coalescence in Inkjet Printing Functional Films: An Experimental Study". In NIP 29: Digital Fabrication 2013, Technical Program and Proceedings, Soc Imaging Sci & Technol; Imaging Soc Japan. 29th International Conference on Digital Printing Technologies, Seattle, WA, Sep 29-Oct 3, 2013.

Author Biography

Dr. Boley received a Bachelor of Science in Mechanical Engineering with a double major in Mathematics from The University of Kentucky in Lexington, KY in May 2006. He continued his studies at The University of Kentucky and earned a Master of Science in Mechanical Engineering in August 2007. Dr. Boley received a Ph.D. in May 2013 from Purdue University in West Lafayette, IN. He currently holds a postdoctoral position at Purdue University.